From mild to wild fluctuations in crystal plasticity

Supplemental material

J. Weiss, W. Ben Rhouma, T. Richeton, S. Dechanel, F. Louchet, L.Truskinovsky

1. Experimental method

Acoustic emission was recorded using piezoelectric transducers directly frozen on the samples (ice), or fastened to the surface of the samples with silicon grease as a coupling material (metals). The frequency bandwidth was 200-750 kHz for ice, 100-600 kHz for monotonic loading of metals, and 125-750 kHz for cyclic loading on Al. Pre-amplification was set to 40dB for ice tests and monotonic loading of metals, and 60 dB for cyclic loading of Al. Detection of AE bursts was performed using a threshold of 30 dB for ice and the monotonic loading of metals and 34 dB for cyclic loading of Al. This ensured an absence of detected bursts when the sample is unloaded (monotonic tests) or cyclically deformed in the elastic domain (Al). Detection time constants (peak definition time, hit definition time, lock-out time) were determined from standard pencil lead breaking Nielsen tests.

2. Acoustic emission source models

Suppose that $A(t)$ is the acoustic signal amplitude (in V). The power of the AE averaged over a time window Δt is defined as

$$\left.\frac{dE}{dt}\right|_{\Delta t} = \frac{1}{\Delta t}\int_t^{t+\Delta t} A^2(t)dt.$$

The continuous AE is defined as the acoustic power sampled over time windows Δt large (10ms – 1s) compared to the duration δt of detected individual bursts (0.1 ms – 10 ms). Hence, it includes experimental noise and, possibly, the AE energy of individual bursts arising during the time Δt. Individual bursts are detected when $A(t)$ passes a defined threshold A_{th} which must be larger than the amplitude of the experimental noise.

Standard AE recording systems can automatically determine several characteristics of the waveforms such as: the duration δt, the maximum amplitude A_0, which is reached right after threshold passing (the rise time is small compared to burst duration), or the AE energy E (Figure S1)

$$E = \int_t^{t+\Delta t} A^2(t)dt \,.$$

The goal of AE source models is to relate these characteristics to the properties of the source(s), i.e. to the motion of dislocations in the present case.

In addition to the recording of the continuous AE and the bursts, we also recorded raw AE signal $A(t)$ sampled at frequencies larger than the resonance frequency of the AE sensors, i.e. at 5 MHz. This allowed us to check the validity of the source model used to interpret the continuous AE, and particularly the Gaussian nature of the signal and the absence of intermittency (see below). For technical reasons, such high-frequency sampling was performed only during limited time windows (e.g. individual loading cycles in case of cyclic loading of aluminum).

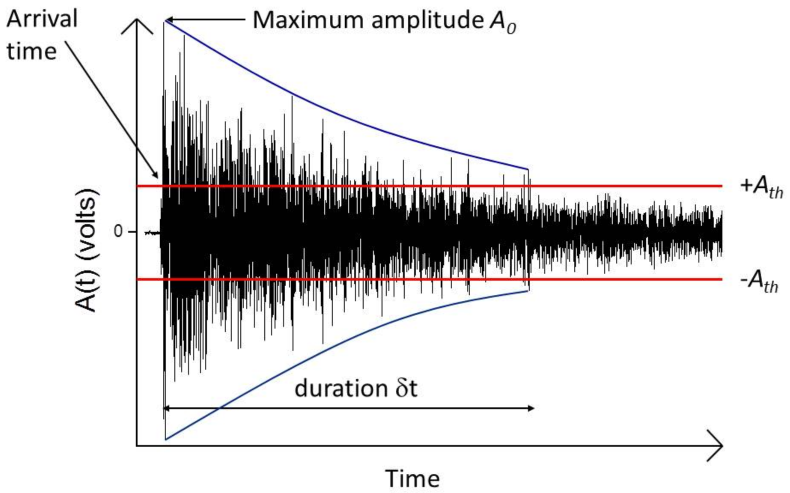

Figure S1. A typical acoustic burst and the definition of the arrival time, the maximum amplitude A_0, and the duration δt.

2.1 AE source model for individual bursts

The source model used to interpret the "discrete" AE (bursts) is based on the analysis of Rouby et al.[*Rouby, et al.*, 1983, 1983]. The main hypotheses and characteristics of this model have been already discussed elsewhere [*Richeton, et al.*, 2005, *Weiss, et al.*, 2000, *Weiss, et al.*, 2007], and are summarized below.

The basic assumption is that an AE burst results from the *transient* and *synchronized* motion of n dislocations constituting a dislocation "avalanche". By *synchronized*, we mean that the average time delay τ between the triggering of individual dislocation motions *within the avalanche* (e.g. between dislocations i-1 and i) is small compared to the characteristic period of the AE transducer, 1/ω, where ω is the frequency. For a typical value ω=200 kHz, it means τ<5μs. In the context of an avalanche-like process, where the onset of the motion of dislocation i might partly result from dynamic triggering associated with dislocation i-1, the distance between dislocations i-1 and i is necessarily smaller than $\tau \times C_S$, where C_S is the shear wave speed. Taking C_S ≈2000 m.s^{-1} for ice and τ=1μs, we obtain a distance of 2 mm, which is very large compared to the average distance between dislocations (~ 100 nm - 1 μm). In most cases, τ is probably much smaller than 1 μs, of the order of nanoseconds. Note that the duration of the avalanche, and so of the corresponding AE burst, can be much larger than τ (or $1/\omega$) as individual dislocations can move during a timescale much larger than τ, and n can be very large.

In a crude model, straight dislocations of length l move with a variable velocity $v(t)$ during the plastic event. They are assumed static ($v = 0$) before and after the event. Making low frequencies ($\omega < 10^6$ Hz) and far field (distance source-transducer significantly larger than l) assumptions, and considering the case of a piezoelectric transducer responding to surface velocity, one can relate the amplitude of the acoustic wave $A(t)$ to the total dislocation length $L = nl$ and the velocity v[*Richeton*, 2006, *Richeton, et al.*, 2005, *Rouby, et al.*, 1983]:

$$A(t) \sim bLv(t) \qquad (S1)$$

Among the assumptions listed above, the far field assumption might be possibly questioned for very large avalanches that span a significant proportion of the system cross-section [*Weiss, et al.*, 2007]. The term $Lv(t)$ accounts for the surface S swept in a unit of time by dislocations during the avalanche, therefore

$$\frac{dS}{dt} = Lv.$$

When multiplied by the Burgers vector b and normalized by a volume (e.g. the sample volume), this term represents a strain rate $d\varepsilon_p/dt$. As noted above, only the maximum amplitude A_0, which roughly corresponds to the amplitude at the initiation of the plastic event, is measured by AE recording systems. An additional hypothesis on the decay of $v(t)$ is therefore needed to estimate the strain increment ε induced by the avalanche. As in most cases where friction is involved, one can assume an exponential decay with time for the velocity, i.e. of the equivalent strain-rate:

$$v(t) = v(t_0)\, exp[-\alpha(t - t_0)] \qquad (S2)$$

where $t = t_0$ represents the onset of the avalanche where the amplitude is maximum, i.e. $A_0 = A(t_0)$ (in good agreement with the recorded waveforms), and α is a damping coefficient. Then, by integrating (S1) over time, we obtain an AE source model which relates directly the value of the maximum amplitude of the acoustic wave to the surface swept out by dislocations during the avalanche, and so to the corresponding strain increment ε_p:

$$A_0 \sim \alpha Sb \sim \alpha\varepsilon_p \qquad (S3)$$

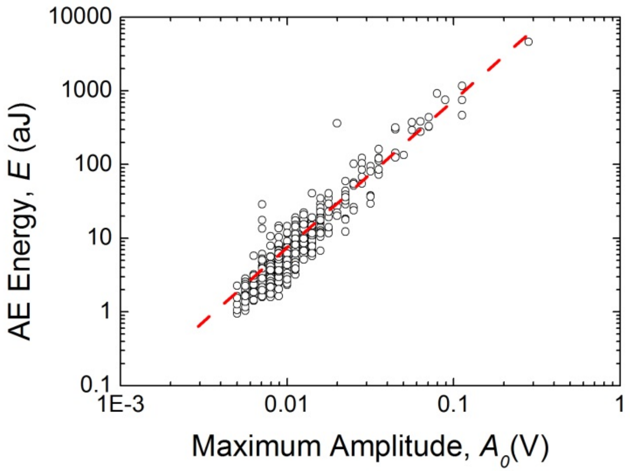

Figure S2. Relationship between the maximum amplitude A_0 and the AE energy E of AE bursts detected during the cyclic loading of a polycrystal of Aluminum ($\varepsilon_{min}/\varepsilon_{max}$=-1, 0.1 Hz, $\Delta\varepsilon = 0.95\%$, T=20°C). The red dashed line represents the scaling $E \sim A_0^2$.

The decay hypothesis (S2) is validated by the following observations:

(i) It implies a relationship between the burst's duration δt and A_0, $\delta t \sim \frac{log(A_0)}{\alpha}$, which is observed experimentally for more than 98% of the events, and not respected only for the largest ones [*Richeton, et al.*, 2005, *Weiss, et al.*, 2007]. Indeed, in this last case, the acoustic signal may remain above the fixed threshold for the period of time between the "mainshock" and several "aftershocks", thus merging distinct events into an anomalously long single one.

(ii) Such decay also implies a simple scaling between the AE amplitude A_0 and the AE energy $E = \int_t^{t+\delta t} A^2(t)dt \sim \frac{A_0^2}{2\alpha} \sim A_0^2$, which is also observed (Figure S2).

(iii) For materials where wild fluctuations associated with individual AE bursts account for most of dislocation motion, such as ice, relation (S3) implies that, when averaged over a large enough time window Δt encompassing a statistically representative population of events, the rate of AE activity should scale with the macroscopic plastic strain-rate, $\frac{\sum_{\Delta t} A_0}{\Delta t} \sim \frac{d\varepsilon_p}{dt}$. This has been observed experimentally [*Weiss and Grasso*, 1997].

In conclusion, in the case of discrete AE, the maximum amplitude of an AE burst, A_0, or alternatively $E^{1/2}$, is a measure of the incremental strain associated with the dislocation avalanche.

2.2 AE source model for continuous AE

The fundamental hypothesis behind the interpretation of continuous AE is that plastic deformation results from the cumulative effect of *numerous uncorrelated* (in space as well as in time) *small* motions, corresponding to dislocation sources activated in independent "units" having a similar size, such as dislocation sub-structures [*Fleischmann, et al.*, 1977, *Rouby, et al.*, 1983, *Slimani, et al.*, 1992]. The waiting times between the successive small motions will be, in average, larger than 1/ω but smaller than the sampling period of continuous AE (10 ms $\leq \Delta t \leq$1s). In this case, the independent but similar AE sources are characterized by a dislocation sweeping area of mean value $\bar{S}$. As above (see S3), we consider that the elastic wave amplitude generated by an individual source scales as:

$$A_0 \sim b\bar{S}$$

However, in the present case, as many independent sources are assumed to overlap, AE energies instead of amplitudes sum up, and the AE power scales as [*Chicois, et al.*, 1986, *Kiesewetter and Schiller*, 1976, *Slimani, et al.*, 1992]:

$$\frac{dE}{dt} \sim \frac{dN}{dt} b^2 \bar{S}^2 \tag{S4}$$

where $\frac{dN}{dt}$ is the number of sources activated per unit time. Hence, we obtain:

$$\frac{dE}{dt} \sim b\bar{S}\,\frac{d\varepsilon_p}{dt} \tag{S5}$$

as

$$\frac{d\varepsilon_p}{dt} \sim (b\bar{S})\,\frac{dN}{dt}.$$

So, if the underlying hypotheses are correct, the continuous AE should not exhibit any intermittency, and the associated AE power should scale as the macroscopic plastic strain-rate. We show below that these expectations are indeed verified.

3. Analysis of the raw AE signal

During the cyclic loading tests on aluminum, the raw AE signal was recorded at 5 MHz over some time windows. We analyze below a 0.1 s time window (i.e. 5×10^5 data points) recorded near the maximum of continuous emission during the loading cycle, just after macroscopic plastic yield, for cycle 329 of a strain-control test, see Figure 3 of the main text. The signal amplitude was squared to obtain the corresponding AE power.

To check the absence of intermittency of this AE power, we performed a multifractal analysis [*Lebyodkin, et al.*, 2009]. This was done for (i) a 0.1 s time window recorded before the onset of loading (with the aluminum sample and the AE transducers in place) and (ii) for the signal sampled at plastic yield (see Figure 3a). The partition functions of order q of the signal are calculated, $S_q(\Delta t) = \sum_i \mu_i{}^q$, where the local probability measure of the ith interval $\mu_i(\Delta t)$ is defined as the sum of the signal within the interval, normalized by the total sum over the entire 0.1 s window. This is done for various time scales Δt, and various values of q. If the signal is multifractal, one has $S_q(\Delta t) \sim \Delta t^{(q-1)D_q}$, with *D(q)* the generalized fractal dimensions. Such multifractal scaling was obtained for an AE signal recorded during the jerky flow (Portevin – Le Chateliereffect) of an Al-Cu alloy loaded under monotonic loading. It revealed the scale-invariant intermittency of plastic flow in this case [*Lebyodkin, et al.*, 2009].

Instead, if the signal is a pure white noise, one should have $\log(S_q)/(q\text{-}1) \sim \Delta t$, whatever q. Any departure from this scaling might indicate some time clustering. The results for q=1.5, 2, 3, 4 and 5 are shown on Figure S3. Other results for other cycles and/or other tests are very similar.

A slight departure from the theoretical white noise scaling is observed below 100 µs. However, the same departure is observed before and during loading, meaning that it is an experimental artifact (AE transducers, environmental noise, etc.). We can therefore conclude in the absence of detectable time clustering. Combined with the Gaussian distribution of extrema (see Figure 3b of main text), this demonstrates the Gaussian white noise character of the AE signal, in agreement with a plastic flow occurring through small uncorrelated motions. We can note that if the same analysis is performed over a time window comprising one or several detected AE bursts, the departure from the white noise scaling and/or the pre-loading situation is pronounced (not shown).

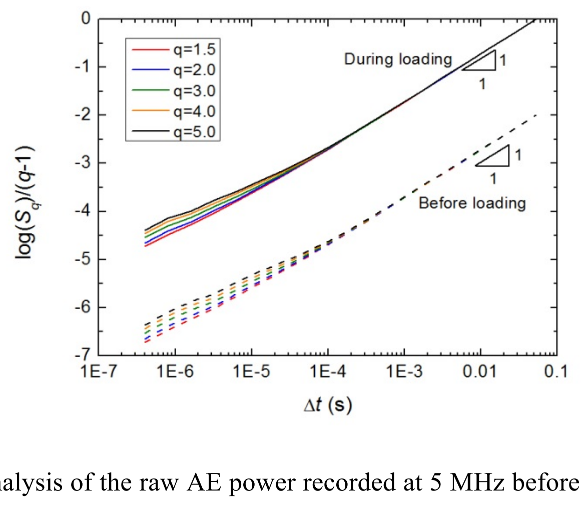

Figure S3. Multifractal analysis of the raw AE power recorded at 5 MHz before (dashed lines), and during (solid lines) loading.

4. Validation of the continuous AE source model

The absence of intermittency of the raw AE signal is in full agreement with the underlying hypotheses of the source model detailed in section 2.2. In the same section, we stressed that the corresponding AE power should scale as the macroscopic strain-rate. This correspondence can be checked directly from AE and strain measurements (extensometry). In case of cycling loading of Al, the agreement is surprisingly good, either for strain- or stress-control tests for loading cycles within the saturation stage, i.e. when the intermittent component of plasticity is minimal (Figure S4a&b). In this analysis, during a given loading cycle, the area swept by the dislocations in the cells, $\bar{S}$, in (S4) or (S5), is considered to be constant during one loading cycle. Indeed, if the dislocation sub-structure is known to evolve from one cycle to another, especially during the first ones corresponding to macroscopic strain hardening [*Videm and Ryum*, 1996], the associated characteristic cell size is not expected to significantly evolve within a cycle during the saturation stage. This way, the evolution of AE power just follows $\frac{dN}{dt}$. The same correspondence $\frac{dE}{dt} \sim \frac{d\varepsilon_p}{dt}$ was previously observed for the monotonic loading of Al [*Kiesewetter and Schiller*, 1976].

On the other hand, as noted in the main text, power law distributed AE bursts occur from time to time and superimpose on the continuous AE. These bursts are particularly frequent during the first few loading cycles. This can be understood by a dislocation sub-structure not yet fully formed at this stage [*Videm and Ryum*, 1996]. Strain hardening is observed during the first few tens of cycles and represents a signature of the formation of the sub-structure. In this case, the plastic strain-rate only follows the continuous component of the AE power (Figure S4c).

One important point should be stressed: if the "continuous" AE averaged over a large time window Δt was the result of the cumulative effect of *individual*, *non overlapping* (as in section 1.1) but *undetected* bursts, the AE power should scale as $\frac{dE}{dt} \sim \left(\frac{d\varepsilon_p}{dt}\right)^2$ instead, which is not observed.

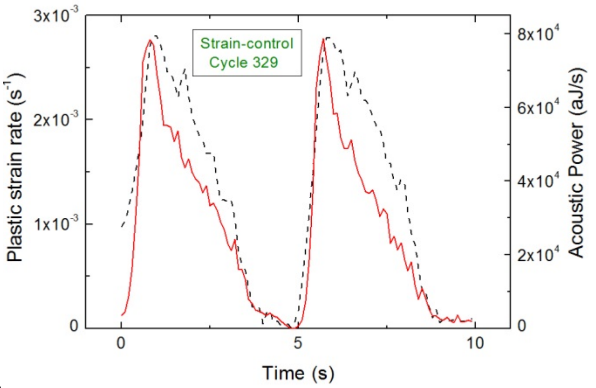

a)

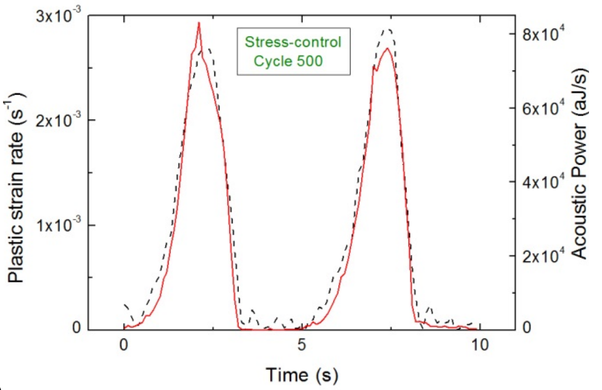

b)

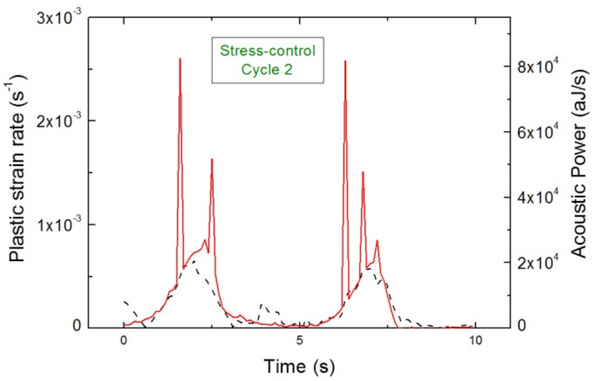

c)

Figure S4. Comparison between the AE power, sampled at 10 Hz and recorded during the tension-compression cyclic loading of aluminum samples (red solid lines), and the macroscopic strain-rate measured by extensometry (dashed black lines). (a) Strain-control test ($\varepsilon_{min}/\varepsilon_{max}$=-1, $\Delta\varepsilon$ = 0.95%, T=20°C, cycle 329). (b) Stress-control test ($\varepsilon_{min}/\varepsilon_{max}$=-1, 0.1 Hz, $\Delta\sigma$=62 MPa, T=20°C, cycle 500). (c) idem as (b) but for cycle 2. The environmental background noise has been removed from the recorded AE power.

5. Contribution of detected AE bursts to the total acoustic power

Material	Loading mode and conditions	% of AE Power explained by detected bursts
Ice (single crystals)	Compression creep (0.15 MPa $\leq\sigma_I\leq$0.56 MPa) T=-10°C	99.95 to 100
Ice (single crystal)	Increasing compression creep stress ($\dot{\sigma}_I$= constant); T=-10°C	100
Ice (polycrystals; mean grain size = 0.87 mm)	Compression creep (0.09 MPa $\leq\sigma_I\leq$0.54 MPa) T=-10°C	98 to 99.95
Ice (polycrystals; mean grain size = 1.92 mm)	Compression creep (0.09 MPa $\leq\sigma_I\leq$0.54 MPa) T=-10°C	99.95 to 100
Ice (polycrystals; mean grain size = 5.02 mm)	Compression creep (0.08 MPa $\leq\sigma_I\leq$0.55 MPa) T=-10°C	99.9 to 100
Cadmium (single crystals)	Uniaxial tension (1.33 10^{-3} $s^{-1}\leq\dot{\varepsilon}\leq$6.7 10^{-3} s^{-1})	96.5 to 100
Zn0.08%Al (single crystal)	Uniaxial tension ($\dot{\varepsilon}$=1.3 10^{-3} s^{-1})	98
Copper (single crystals)	Uniaxial tension (5.1 10^{-3} $s^{-1}\leq\dot{\varepsilon}\leq$1.9 10^{-2} s^{-1})	11 to 58
Cu7.5%Al (single crystal)	Uniaxial tension ($\dot{\varepsilon}$=3.9 10^{-3} s^{-1})	1.5
Cu10%Al (single crystal)	Uniaxial tension ($\dot{\varepsilon}$=3.8 10^{-3} s^{-1})	1.5
Cu15%Al (single crystal)	Uniaxial tension ($\dot{\varepsilon}$=3.3 10^{-3} s^{-1})	9
Aluminum (single crystals)	Uniaxial tension (8 10^{-4} $s^{-1}\leq\dot{\varepsilon}\leq$3.6 10^{-3} s^{-1})	1.5 to 2.5
Aluminum (polycrystals)	Cyclic tension-compression Strain control (R_{ε}= -1) (0.5%$\leq\Delta\varepsilon\leq$1.5%)	~10^{-4} % globally From 0 to few % depending on the loading cycle

Aluminum (polycrystals)	Cyclic tension-compression Stress control (R= -1) (50MPa≤$\Delta\sigma$≤62MPa)	~10^{-4} % globally From 0 to few % depending on the loading cycle

Table S1. Contribution (in %) of the detected AE bursts to the total AE power measured above the experimental background noise, for various materials and loading configurations.

6. Stochastic trajectories

In Figure S5 we illustrate the structure of the fluctuations of the average dislocation density generated by Eq. (1) at a = 1, c = 1, and different values of noise intensity D. The histograms showing size distributions of the avalanches are plotted in the insets. The calculations were performed by using a Milstein iterative scheme and averaging was done over 10^5 stochastic realizations.

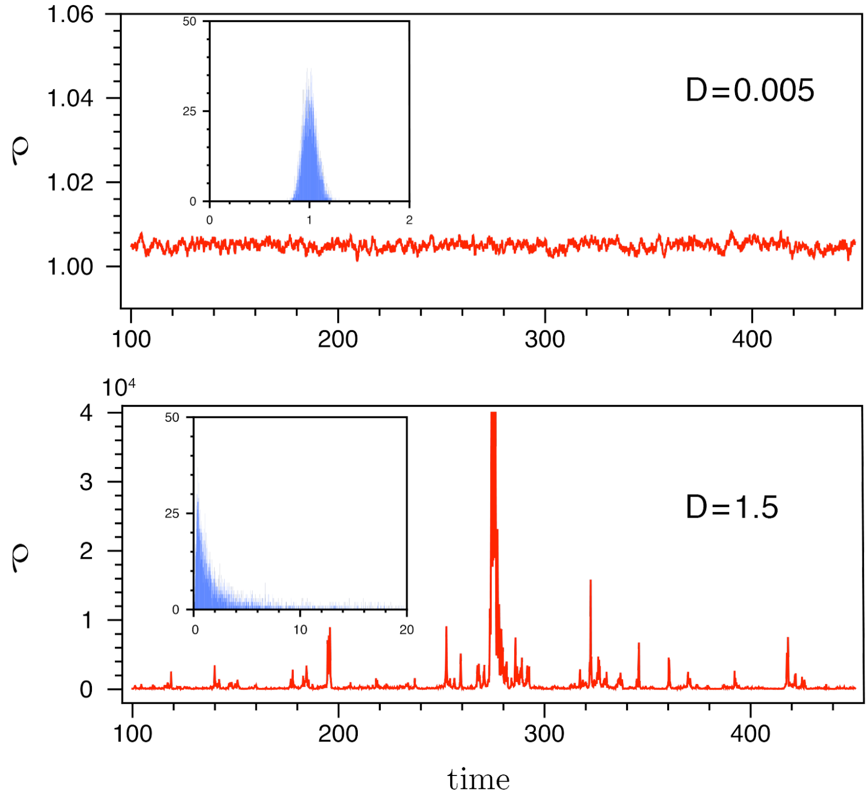

Figure S5. Typical stochastic trajectories generated by Eq. (1).

References

Chicois, J., et al., *Acta Metallurgica*, **34**(11), 2157 (1986)
Fleischmann, P., et al., *Mat. Sci. Eng.*, **29**, 205 (1977)
Kiesewetter, N. and P. Schiller, *Phys. Stat. Sol.*, **38**, 569 (1976)
Lebyodkin, M. A., et al., *Phys. Rev. B*, **79,** 174114 (2009)

Richeton, T. (2006), Dynamique et complexité de la déformation plastique: Etude par émission acoustique, PhD Thesis, INP Grenoble, Grenoble.
Richeton, T., et al., *Acta Materiala*, **53**, 4463 (2005)
Rouby, D., et al. *Philosophical Magazine A*, **47**(5), 671 (1983)
Rouby, D., et al. *Philosophical Magazine A*, **47**(5), 689 (1983)
Slimani, A., et al., *J. Phys. III France*, **2**, 933 (1992)
Videm, M. and N. Ryum, *Mater. Sci. Eng. A-Struct. Mater. Prop. Microstruct. Process.*, **219**(1-2), 1 (1996)
Weiss, J. and J. R. Grasso, *J. Phys. Chem. B*, **101**, 6113 (1997)
Weiss, J., et al., *J. Geophys. Res.*, **105**(B1), 433 (2000)
Weiss, J., et al., *Phys. Rev. B*, **76**, 224110 (2007)